JOURNAL OF AIRCRAFT
Vol. 44, No. 5, September–October 2007

Lift and Drag Characteristics of a Blended-Wing Body Aircraft

David A. Gebbie* and Mark F. Reeder†
Air Force Institute of Technology, Wright–Patterson AFB, Ohio 45433
Charles Tyler‡
U. S. Air Force Research Laboratory (AFRL/VAAC), Wright–Patterson AFB, Ohio 45433
and
Vladimir Fonov§ and Jim Crafton¶
Innovative Scientific Solutions, Inc., Dayton, Ohio 45440

DOI: 10.2514/1.22356

The aerodynamic characteristics of a blended-wing body aircraft were assessed in the Air Force Institute of Technology low-speed wind tunnel. The scaled-down model ($Re_c \sim 10^5$ and $M = 0.10$ to 0.20) of a strike tanker consisted of a shaped fuselage and slender, sweptback wings. The model evaluation and analysis process included force and moment measurements acquired from a wind-tunnel balance along with complementary pressure sensitive paint measurements and computational fluid dynamics solutions for a few cases. The force and moment coefficient data suggested that the aircraft is affected by both vortex lift and potential flow lift mechanisms. This was manifested in an apparent stall mechanism with a significant dependence on airspeed. One of the most intriguing aspects of the results was the striking difference in the force and moment measurements before and after the paint was applied to the surface. Although the roughness for both models was below the threshold suggested by 2-D boundary layer theory for all data acquired, the application of the paint led to a clear and repeatable effect on the force coefficient data. The lift slope was steeper and the onset of stall, when it occurred, was sudden across the entire wing for sufficiently smooth models. By contrast, the lift slope was reduced and stall was indicated only through a mild change in lift slope for the measurements corresponding to the rougher surface.

Nomenclature

b	=	wing span
C_D	=	drag coefficient
C_L	=	lift coefficient
C_m	=	pitching moment coefficient
C_N	=	normal force coefficient
C_p	=	pressure coefficient
c	=	chord
Re	=	Reynolds number
α	=	angle of attack

I. Introduction

IN THE past few decades, technological advancements have enabled faster and more accurate assessment using three specific methodologies: 1) rapid prototyping, 2) computational fluid dynamic (CFD) modeling, and 3) global measurements. One goal of the U.S. Air Force Research Laboratory Air Vehicle Directorate (AFRL/VA) is to integrate each of these areas with one another so that they function in a complementary manner. The current study was undertaken to apply each of these rapid development technologies for a modern unconventional, rather than a simplified, air frame model. To this end, an industrial air framer provided AFRL with detailed electronic model information to fully define the external strike tanker geometry. A rapid prototype design methodology was developed and used to construct a stainless steel model. The model was constructed using selective laser sintering (SLS) of stainless steel, and several features were incorporated to improve the ease with which wind-tunnel measurements could be completed. For example, built-in pressure taps improved the speed and accuracy of pressure sensitive paint (PSP) measurements. Additional details of the solid model construction procedure are given elsewhere [1,2]. This electronic model was also used as a starting point for constructing the computational grid, and a portion of the project was devoted to comparing experimental and computational results.

The tested model is a variation of a blended-wing body (BWB) design in that the centerbody of the aircraft is designed to contribute to the aircraft's lift. It is envisioned that this type of aircraft could serve in military applications as a tanker with increased capacity, which could be launched with a strike force, eliminating the need to get tanker assets in place before launching bombers [3]. There have been a number of studies performed on the blended-wing body concept, though many of the results are proprietary. Two exceptions describing results for a BWB aircraft are given in [4,5], and each of these is pertinent to the current investigation.

Katz et al. [4] summarized experimentally obtained force and moment coefficient measurements acquired for a specific BWB design at an approximately $Re_c = 4 \times 10^5$, including tests for both wings-on and wings-off data. Their data indicated that the C_L–α curve was linear up to approximately 5 deg, but that a reduction in the slope at that angle existed due to wing stall. It is notable that the C_L–α curve continued to increase throughout the range of the tests, which are shown up to 18 deg. The L/D curve exhibited a peak of approximately 15 in their study, near the break in the C_L–α curve. The pitching moment coefficient data with respect to alpha (C_m–α) showed a slight increase in the slope, consistent with loss of lift aft of the point where the moment coefficient was determined. At larger angles of about 10 deg, there was a reduction in the slope of the C_m–α

Presented as Paper 4719 at the AIAA 23rd AIAA Applied Aerodynamics Conference, Toronto, Ontario (Canada), 6–9 June 2005; received 9 January 2006; revision received 5 September 2006; accepted for publication 16 April 2007.

*First Lieutenant, USAF, currently with AFRL/PRTT, WPAFB, OH. AIAA Member.
†Assistant Professor, Department of Aeronautics and Astronautics, AFIT/ENY, AIAA Member.
‡Research Engineer. AIAA Member.
§Research Engineer. AIAA Member.
¶Research Engineer. AIAA Member.

plot, consistent with a rearward shift in the center of pressure. The results presented in [4] correspond to one airspeed.

A recent study incorporating both CFD and experimental results for a BWB design is summarized in [5]. Pao et al. reported results acquired in the NASA Langley 14 by 22-foot subsonic tunnel for a 33:1 scale model. The tests most pertinent to the current study were of a Mach number range similar to the current set of experiments (approximately $M = 0.2$), but with a much higher Reynolds number —Re_c ranged from 2.6×10^6 to 10^7. An interesting finding was that the experimentally determined normal force coefficient for the 2.6×10^6 case exhibited a small reduction, possibly related to stall, near 23 deg while the measurements corresponding to a higher airspeed ($Re = 3.7 \times 10^6$) showed a more gradual reduction of the normal force coefficient at a smaller α, approximately 20 deg. In contrast to the results given for the BWB studied by Katz, the C_m–α curve exhibited a sharp increase in the slope near 10 deg followed by a decrease near 25 deg. Notably, the result indicating the downward shift in the apparent stall angle, indicated by the break in the C_N–α curve, as the Reynolds number increases, is generally counter to the result expected for a lifting wing [6]. Another relevant disclosure in [5] is that the computational results for the C_N–α curve closely matched the results until α increased above the break, at which point the computational results departed significantly from the experimental data. Those results were obtained using a one-equation Spalart–Allmaras turbulence model.

Although CFD results can provide useful insight into the underlying fluid mechanics leading to lift and drag measurements, experimental validation of the assumptions made in the computations is very helpful, particularly in complex geometries. Because a large portion of CFD predictions of lift and drag are based on integrated surface pressure, experimentally determined surface pressure maps are very useful in this regard and were sought in the current study. PSP was used in the current study, and the general procedure for using PSP is well documented in the literature [7–9].

One of the beneficial aspects of PSP is that no additional intrusive tubes or wires are required for the tests. Rather, a paint coating is applied, and it is typically very thin. Whereas the coating thickness is generally negligible in comparison to the thickness of an aircraft component, the paint could conceivably be a significant source of intrusion if the surface roughness of the model is affected. Several experiments of special pertinence to the current study were dedicated to the study of paint intrusiveness in the testing environment.

A comprehensive study of the intrusiveness of PSP was documented by Schairer et al., who tested a swept wing at high and low Reynolds numbers [10]. They found that at high Reynolds numbers ($Re = 6.7 \times 10^6$), the roughness due to the paint coating changed the pressure distributions near stall and poststall. However, at low Reynolds numbers the paint intrusiveness was quite small and indistinct, which the authors attribute to the paint being sufficiently smooth to remain below the threshold of admissible roughness. In each case, the prestall lift slope was generally unaffected by the roughness. This set of results was consistent with the classical admissible roughness criteria, which is based on two-dimensional boundary layer flow, as documented by Schlichting [11]. Roughness levels for the painted models varied from average roughness (Ra) between 0.5 and 1.5 μm while that of the smooth models was an order of magnitude smaller.

Vanhoutte et al. [12] conducted a low and a high subsonic speed study on swept wings using PSP. They found that at high Reynolds numbers ($Re = 6.0 \times 10^6$), the roughness due to the paint coating could result in a small increment in drag. However, at low Reynolds numbers ($Re = 3.0 \times 10^5$) the paint intrusiveness was small in the linear region of the lift curve but did change the pressure distribution and drag near stall and poststall. In particular, Vanhoutte et al. indicated that the paint roughness near the leading edge influenced the behavior of the separation bubble, possibly removing it altogether, and speculated that the roughness may have also induced crossflow transition, which is a predominant issue in swept wing applications.

Amer et al. [13] documented paint intrusiveness by investigating a delta wing geometry at Mach 0.2. Their results indicated that PSP had little influence on its measured lift and drag values when the paint roughness corresponded closely to the roughness of the original model for the geometry and flow conditions of their tests, which were conducted for Reynolds numbers on the order of 10^7. Their roughness levels were between 0.2 and 1.0 μm.

The more general topic of the effect of surface roughness on the transition to turbulence in swept wing flows is itself an area of current interest [14]. One matter of significance to the current investigation is brought out by Radeztsky et al. [15], who found through flow visualization that even at Reynolds numbers over 10^6, there were distinguishable differences in the transition characteristics of the flow over a swept wing depending on whether the measured roughness was 0.25 or 0.5 μm. This value is substantially lower than the admissible roughness criteria based on two-dimensional flow.

II. Procedures and Methodology

A. Experimental Methods

The rapid prototyping process of the strike tanker used in this experimental study began with a detailed electronic model, as seen below, provided to the University of Dayton Research Institute (UDRI), which was the lead organization for producing the prototype. The combined restrictions of the wind-tunnel dimensions and balance range limited the wing span of the model to a 1/72 scale. Currently available SLS equipment capped the maximum part size at 10 in. by 10 in. by 10 in., resulting in the fabrication of the strike tanker model consisting of six pieces: forward and aft fuselage, left and right wings, and left and right tail fins. Ultimately, the model was assembled from the stainless steel parts shown in Fig. 1. Care was taken to build in aft clearance for the wind-tunnel mounting fixtures, and pressure taps with connecting tubes were built into each wing.

Once it was fully assembled, the surface was polished, and silicone rubber was used to fill seams between the parts. The completed model is shown mounted on the balance in the wind tunnel in Fig. 2. The strike tanker model used had a 20.125 in. wing span with a 25 deg rearward sweep angle while the split v tail had an overall span of 9 in. with the same sweep angle as the wing. The body of the strike tanker was 4 in. wide with an overall length of 16 in. The original length from the leading to trailing edge for the wing and tail were

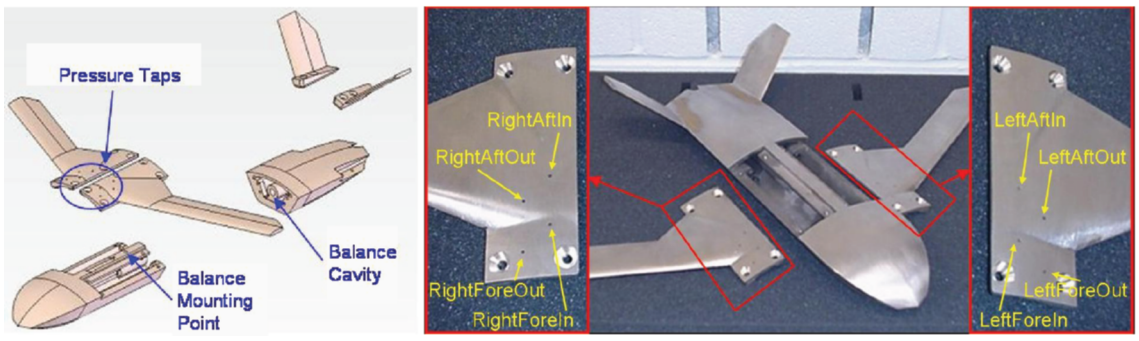

Fig. 1 Model configuration is given in its formative phase (left) and as the model assembly. Pressure tap locations and nomenclature are noted.

Fig. 2 Model configuration mounted in the AFIT low-speed wind tunnel.

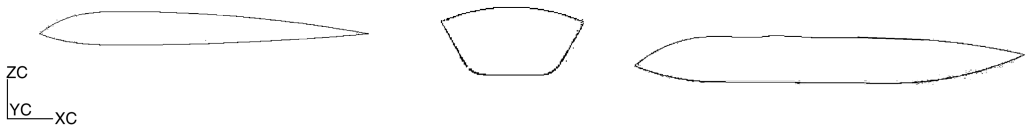

Fig. 3 Two-dimensional cross sections of the model are presented. At the left is the chord of the wing, in the center is a cutaway front view of the body just fore of the wing body junction, and at the right is a cutaway view of the centerline cross section.

1.69 in. and 2.14 in., respectively. As a result the true chord of the wing was 1.86 in. A reference area of 147 in.^2 based on the projected area of the model was used.

The shape of the wing sections and body shape are shown in more detail in Fig. 3. The maximum thickness of the wing section is 10% of the chord, and notably, both the wing section and the body centerline include a sharp leading edge (nose radius less than 0.05 in.). The sharp leading edge has some advantages in a compressible flow environment but has long been known to lead to leading edge stall at relatively low angles of attack. For example, Cahill et al. and Hoerner and Borst [16,17] describe a number of experiments in which stall onset occurs at an angle of attack between 8 and 9 deg for a sharp edge circular arc and diamond shaped airfoil with a maximum thickness of 10% of the chord. Hoerner and Borst [17] present data for a NACA 64A006 airfoil section which demonstrates a mild decrease in the lift coefficient near 5 deg angle of attack and a corresponding mild increase in the section drag coefficient. This type of behavior is consistent with the long bubble type of flow separation on the low-pressure surface of the wing.

Hoerner and Borst [17] also provide some useful insight into the stall behavior of swept wings in that stall onset is shown to be delayed for a NACA 0012 section set at a sweep angle. Generally speaking, for a given uniform airfoil section, stall onset begins near the wing tips and works gradually inward toward the fuselage as the angle of attack is increased. However, it should be emphasized that this generalization does not necessarily hold for BWB air frames. In the case of a delta wing, the lift mechanism changes from purely potential flow lift to vortex lift, as described in [17], as the vortex generated at the leading edge of a delta wing is rotated to a position above the upper wing surface.

The strike tanker model was mounted in the Air Force Institute of Technology (AFIT) low-speed wind-tunnel test section of 31.5 in. (height) by 44 in. (wide) by 72 in. (long). The strike tanker span-to-tunnel width ratio (b/w) of 0.45 falls well under the acceptable ratio according of $b/w < 0.8$. The Plexiglas side doors and top panel provided optical access. The model support sting entered the test section through a slot in the traverse plate at the bottom of the test section. The sting traverse system allowed for angle of attack measurements from -25 deg to $+25$ deg, as well as sideslip angles from -25 deg to $+25$ deg. The sting mounted balance used to collect the force and moment data for the strike tanker was a one-half in. diameter Able Corporation Series D, MKII nominal 100-lb_f, six-component internal strain gage balance, accurate to 0.25% of full capacity. The capacity specifications of the strain gage rosettes are listed in Table 1, and the calibration was checked and confirmed before its installation. Hot-wire anemometry indicated a turbulence intensity of nominally 0.5% for the range of conditions used in this experiment, and additional details of the wind tunnel and mounting configurations are given in [18,19].

The force and moment signals were conditioned and collected using a National Instruments LabView Virtual Instruments interface throughout the test program, and the force and moment coefficients were determined after each set of tests. The chord at the wing body junction served as the length scales used to normalize the pitching moment coefficient. The data were subsequently processed with an in-house MATLAB code, which incorporated a model tare and implemented small corrections due to the wall effects and solid model blockages. Details of the data processing methodology are contained in [17,18]. The force and moment coefficient results reported here encompass only tests performed using angle of attack sweeps at zero yaw, collected at speeds of 60, 90, 110, 130, and 145 mph (26.8, 40.2, 49.2, 58.1, and 64.8 m/s, respectively). The unit Reynolds number ranged from $1.8 \times 10^6/\text{m}$ up to $4.4 \times 10^6/\text{m}$ corresponding to Reynolds numbers ranging from 0.8×10^5 to 1.8×10^5. If the length of the fuselage were used as the characteristic length, which is plausible since it contributed to lift, the Reynolds number for the tests in turn would range from 1×10^6 to 2.1×10^6. Each plot given in the results uses airspeed to characterize the test condition.

Pressure maps of the upper surface of the strike tanker were collected using PSP. The PSP setup in this experimental study used a biluminophore PSP from Innovative Scientific Solutions, Inc. (ISSI). The paint was applied at the AFIT model shop, and, notably, no base coat was applied to the model for the series of tests described here. Future testing will incorporate a base coat to reduce noise in the PSP signal. This paint was chosen due to its low temperature sensitivity and its ability to provide compensation for the model displacement relative to the excitation light source, as well as the instability of the light source itself. The Bi-Luminophore PSP is very similar to Uni-FIB, a single layer paint composed of platinum tera (pentafluorophenyl) porphine (PtTFPP) that uses a fluoro/isopropyl/butyl (FIB) binder; however, it uses a reference probe in addition to the signal probe. The biluminophore paint exhibits a pressure sensitivity of 6% per psig and a response time of 0.3 s and its emission spectrum ranges from 500 to 800 nm with a peak at 650 nm with 460 nm illumination at 20 °C. The light sources used to illuminate the model for the strike tanker test condition were in the form of an array of four 2-in. blue

Table 1 Wind-tunnel balance specifications

0.50 Able Mark VI balance specifications	
Normal force—total	100 lbf ± 0.25%
Side force—total	50 lbf ± 0.25%
Axial force	50 lbf ± 0.25%
Pitching moment	52.5 in. · lb ± 0.25%
Rolling moment	15 in. · lb ± 0.25%
Yawing moment	25.5 in. · lb ± 0.25%

light-emitting diode (LED) light sources emitting at a wavelength of 405 nm. A matrix of more than 30 marker points was used to account for the spatial deformation of the model during the data processing.

The intensity images of the PSP during testing were captured using one of two lenses mounted to a 14-bit Cooke PCO Series 1600 charge-coupled device (CCD) camera linked up with ISSI's image acquisition software, OMS Acquire. The biluminophore paint requires that two images be taken at each test condition. The use of a filter wheel is therefore necessary to capture two separate images under the same illumination conditions separated in time. The filter wheel used contained a 645-nm long pass filter for the signal probe and a 550 ± 40-nm bandpass filter for the reference probe. In addition to all of the PSP equipment used for the last set of experimental tests, all of the previously discussed wind-tunnel equipment including the force and moment balance and pressure tap system was used. The pressure at each tap was collected using Endevco 5 psig pressure transducers. For each measurement, the analysis began with the reference image that was acquired at ambient pressures, also known as a "wind-off" image. In addition, a "dark," or background, image was acquired with the lighting system turned off to account for any variations in background room light. The two categories of "wind on" images (one for each filter) collected during the test were processed with reference to the dark image and the wind-off image using commercially available PSP data processing software (ISSI's OMS Lite Version 1.0) to obtain surface pressure plots. The images were aligned using the marker points within the images, and the resulting pressure maps were filtered and smoothed using a Gaussian filter with the maximum half width of the filter set to 10 pixels in each of the two axes. More details of the PSP system and data collection procedure are given in [19].

B. Computational Procedure

CFD analyses were performed using an U.S. Air Force Research Laboratory developed code to determine the pressure distribution over the wing surface. The three-dimensional solutions were obtained with a full Navier–Stokes code. Laminar solutions were acquired and, in addition, a Spalart–Allmaras turbulence model was implemented for several cases. The CFD code is an unstructured, cell-centered, finite volume, Godunov-type solver that has least-squares gradient reconstruction and limiting for second-order spatial accuracy and first-order, point implicit time interpretation. The hybrid grid consisted of 501,300 cells: 372,472 tetrahedral and 128,828 prisms to acquire viscous boundary layer effects. The full test section of the wind tunnel was modeled as part of the grid generation. The mesh spacing near the surface of the CFD model near the model surface was on the order of 10 μm. CFD was performed for multiple angle of attack settings corresponding to a single airspeed.

No effort was made to implement a trip strip, neither in the experiment nor in the computation. Among the reasons for this omission was that it was desired to maintain a common geometry for the experiment and the computation to satisfy the project goal. A second reason was that there is no traditional rule for locating a trip strip on blended-wing body geometries.

III. Results

A. Force and Moment Coefficients

Experimentally measured force and moment coefficients are given here for a variety of test conditions. A number of unexpected results affected the choices made within the data collection process, and for that reason, some reference is made to the chronology of experiments.

The initial set of results obtained for the model is given in Fig. 4. This series of tests was conducted with the intent of checking the strike tanker structural integrity and wind-tunnel measurement system, and as such it was conducted for the model before any paint application. The propagated uncertainty of tests was affected primarily by force balance. Based on the balance accuracy, for which the data were given in Table 1, the level of uncertainty in the lift coefficient at a nominal angle of attack of 6 deg, for example, was approximately 0.02 and the level of uncertainty in the drag coefficient was 0.004. The results were unanticipated in several respects. First, the apparent reduction in C_L, hereafter referred to as the apparent stall event, was not predicted by CFD, nor was it indicated in the work on the BWB described in [4].

The second surprising feature of the lift curve was the strong dependence of the stall angle, indicated by a drop in the lift coefficient, on airspeed. At 60 mph, no stall was seen through $\alpha = 25$ deg while at 90 mph, stall apparently occurred at $\alpha = 21$ deg. Both the magnitude of the apparent stall event and the angle at which it occurred were strongly affected by the airspeed with the angle gradually reduced as airspeed increased such that, at 145 mph, the stall event corresponded to $\alpha = 7$ deg. This effect is the opposite of what one would expect for a typical lifting wing if Reynolds number effects are taken into account. It is noteworthy that the decrease in stall angle with airspeed result is consistent with the findings of Pao et al., though it should be noted that this comparison is based on the authors' presented data of normal force coefficients for only two different airspeeds and Reynolds numbers [5].

Thirdly, the drag coefficient did not show a dramatic increase, generally associated with stall for a wing experiencing potential flow lift. Rather the polar plot simply showed a shift in the drag bucket from a more efficient to a less efficient outcome as angle of attack increased. Furthermore, both the lift and drag coefficients continued to increase with angle of attack, even after this stall event had taken place. Maskell's wake correction was not applied due to uncertainty regarding separation and due to the relatively large ratio of model-to-wind-tunnel span. However, in a typical stall event it is worth noting that a correction applied taking the wake into account would have reduced poststall C_D values even further.

As a consequence of this result, it was deemed appropriate to check the data for repeatability. The model was removed, and several weeks later, data were acquired under similar test conditions. The outcome for this repeatability check was consistent, and one set of repeatability tests is given here in Fig. 5. Given the repeatability of the results, it was deemed appropriate to continue testing with PSP, with focus given to identifying the surface pressure features surrounding the stall event.

It should be pointed out that the initial effort in the course of testing was focused neither on the intrusiveness of PSP nor on the effects of model roughness on forces and moments. For this reason, no roughness measurements were taken for the original model. In retrospect, that type of measurement might have offered some additional insight into the results, as later results indicated.

A set of force and moment coefficient results collected for the painted model are given for the 110 mph test runs in Fig. 6 and for the 145 mph test runs in Fig. 7. The results are compared to those for the original, unpainted model and the 110 mph results are further compared to the original CFD results for both a laminar simulation and for the aforementioned turbulence model. Analysis of the force and moment data suggested that the paint application had apparently affected not only the characteristics surrounding the stall event, but had even had some effect on the lift slope. These measurements more closely matched the CFD results, and the results for the painted model had similar characteristics to those reported in [4]. Specifically, Katz et al. had reported a mild decrease in slope, which was attributed to wing stall, rather than an abrupt reduction in C_L.

The pitching moment coefficient results were quite different for the painted and unpainted model, as shown in Fig. 8. The painted model exhibited mild changes in the slope of the $C_{m\text{-}\alpha}$ curve which was similar to those reported by Katz et al. for their BWB model. By contrast, the results for the unpainted model, which showed a sharp increase at a specific angle of attack, were characteristically similar to that reported by Pao et al. in [5] for a different BWB model. Despite this relation of each data set to archival data, the difference in the character of the two sets of results was surprising, especially because the application of the paint was expected to be relatively unintrusive. In addition, the effect of paint roughness on the lift slope outside of the stall region was not reported in [10,12], which were dedicated to quantifying PSP intrusiveness effects.

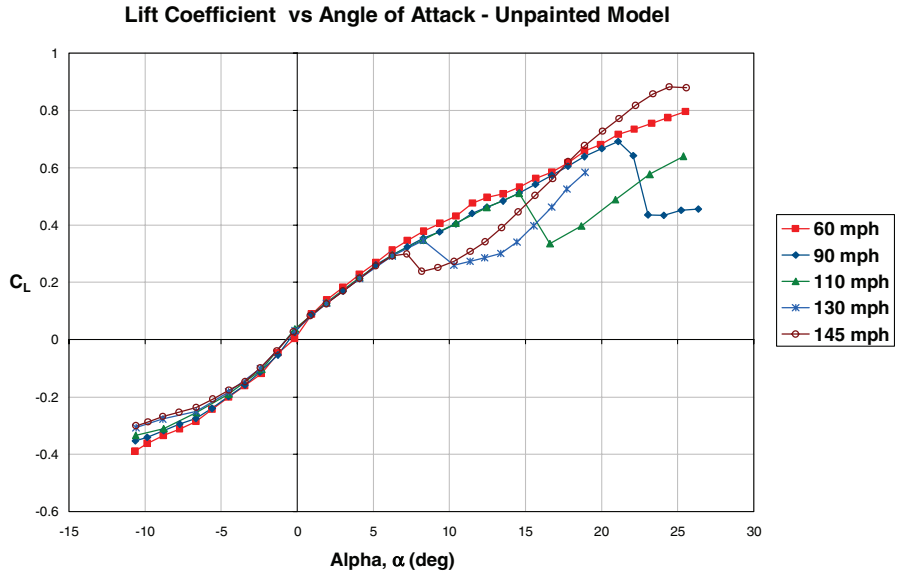

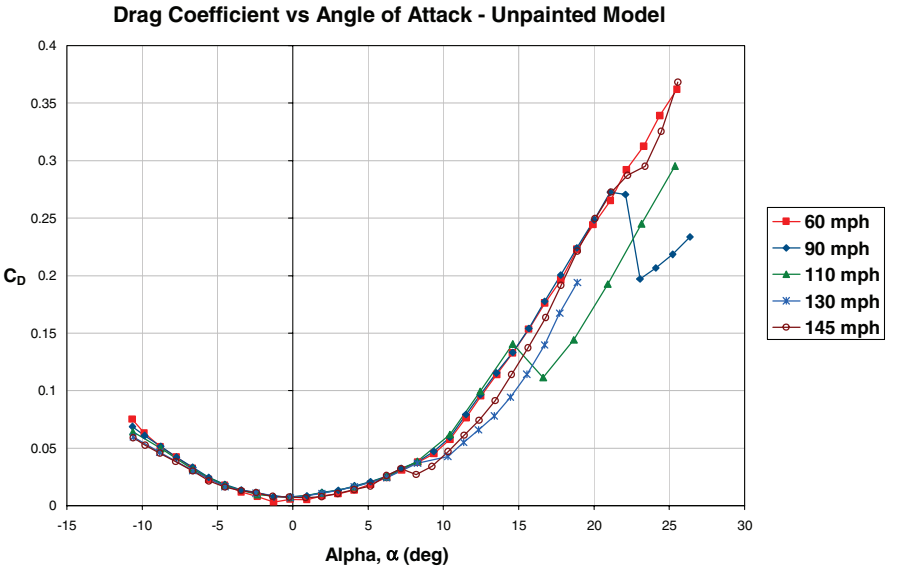

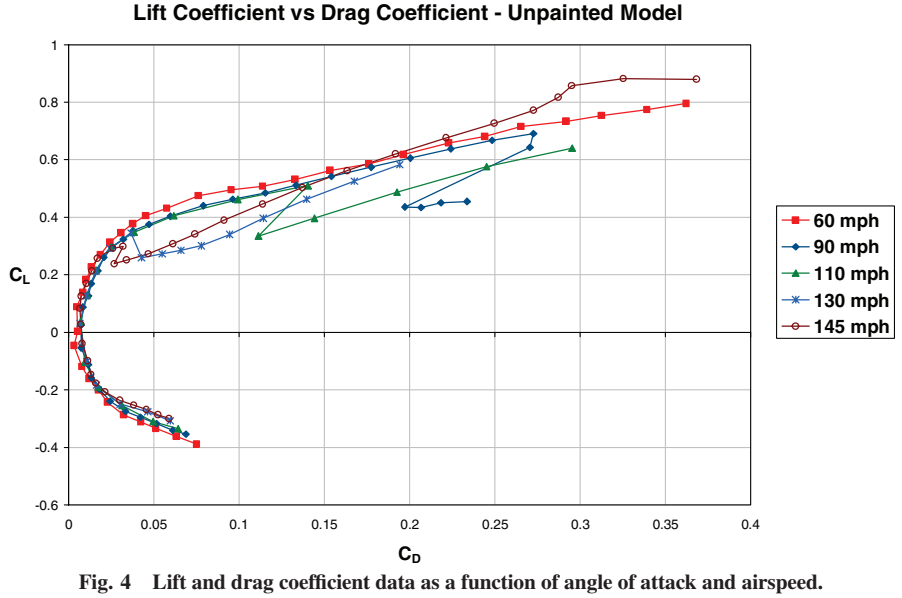

Fig. 4 Lift and drag coefficient data as a function of angle of attack and airspeed.

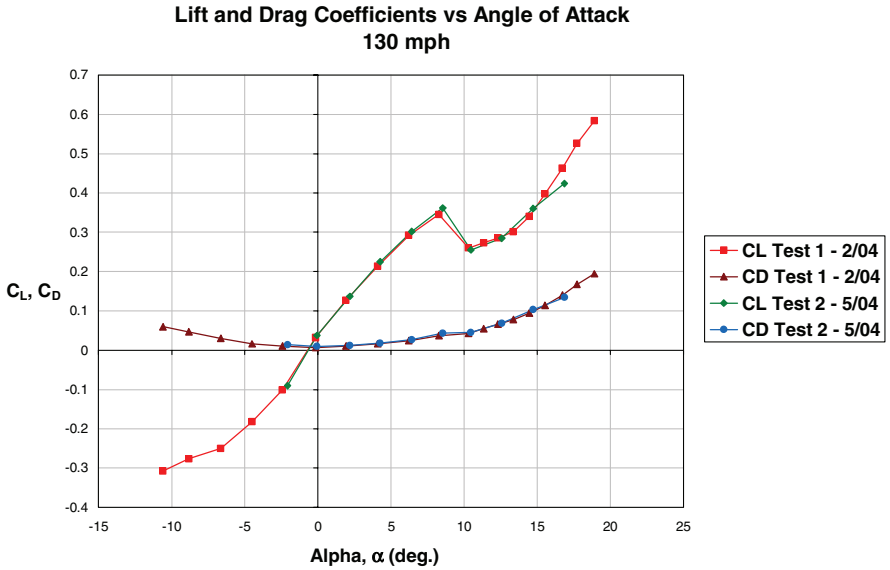

Fig. 5 Force coefficient data as a function of angle of attack.

B. Surface Pressure Comparison of PSP and CFD

The experiments conducted to determine surface pressure maps lent some insight into the flowfield. The eight pressure taps located within the fuselage provided some information for comparison to CFD results while the PSP measurements yielded additional information over the upper surface of the aircraft. Data acquired from one pressure tap location are given in Fig. 9 in terms of the pressure coefficient as the angle of attack was varied. This tap location (right, fore, outer as shown in Fig. 1) provided a useful, in situ reference pressure for PSP, in part because the region was not strongly affected by either airspeed and varied relatively smoothly with α. It should be noted that each of the pressure taps, all located inboard of the wing body junction, indicated a monotonic decrease of pressure as angle of attack increased. Because of model geometry constraints, no pressure taps were located along the wings themselves. Notably, this pressure tap showed similar pressure coefficients for both the 110 and 145 mph cases.

Side-by-side PSP and CFD results are given in Fig. 10 for the 110 mph test case at α corresponding to 8, 12, and 16 deg for the painted model. Note the slight difference in the color scale for each figure. As one would expect, a wider pressure range was measured for the higher airspeed condition. Additional results for these specific test conditions are given in [19]. An additional PSP plot for the 145 mph case with the pressure scale adjusted to reflect the lower range of measured pressures is given in Fig. 11. The accuracy of PSP tests in a low-speed wind-tunnel environment has been estimated to be approximately 0.01 psi by Bell [9]. This value can be affected by many factors such as the type of camera, paint, etc. In this instance the value of uncertainty of 0.01 psi is a reasonable estimate, given the use of independent reference pressures in combination with the camera and illumination system.

Consistent with potential flow lift, there was a reduction in the pressure near the leading edge of each wing for both speeds up to and including the 8 deg case. Ambient pressure was 14.18 psia. For the 110 mph case, the reduction was from approximately 13.9 to 13.6 psia while the 145 mph case showed a reduction from approximately 13.6 to 13.2. However, the low-pressure region near the leading edge of the wings was diminished between the 8- and the 12-deg angle of attack test cases. Arguably, this low-pressure region was slightly more intact at 12 deg for the 110 mph case than for the higher speed case. As the angle of attack increases the wing apparently stalls and a low-pressure region forms near the wing body junction. This appears to indicate that a streamwise vortex lift system may have developed at these higher angles of attack, and this is a major contributor to the lift for the vehicle at higher angles of attack.

Though not wholly satisfying in that the force coefficients changed with the application of the paint, the pressure contour plots do lend some insight into the force coefficient data. With reference to Figs. 6 and 7, it can be seen that the $C_{L-\alpha}$ for the painted model differs substantially from that of the unpainted model. For the unpainted model, there was a clear stall event which transpired at a relatively low angle of attack, with considerable dependence on the freestream velocity. The lift curve for the painted model exhibits three approximately linear regions. The first region extends to approximately 6 deg, the second from about 6 to 15 deg, and the third being above about 15 deg. The PSP and CFD results likewise revealed that between 6 to 15 deg, a transition from leading edge suction (potential flow lift) along the wing to vortex lift near the wing body junction takes place. The PSP clearly indicates that for angles greater than 15 deg, the low-pressure region near the wing body junction is a primary contributor to lift. These regions are slightly more pronounced for the 145 mph case than for the 110 mph case, but are present at each speed. The plots of surface pressure based on the CFD simulation employing the Spalart–Allmaras turbulence model showed a similar trend as the angle of attack was increased from 8 to 16 deg. The low-pressure region near the leading edge of the wing diminished as a broader low-pressure region near the wing body junction grows. However, even at 16 deg angle of attack, the low-pressure region appears to be intact for both wings.

A plausible explanation for this behavior is that the paint application affected the development of the leading edge long bubble separation. The data suggest that whatever the nature of the development of the bubble was for the unpainted model (occurring at about 15 deg for the 110 mph case and at about 7 deg for the 145 mph case), the application of the paint caused the event to become more gradual, taking place over a range of values of the angle of attack before settling to a similar outcome at higher angles of attack. Questions left unanswered by this set of PSP and CFD data include where and how the long bubble stall takes place, even for the painted model. Furthermore, it was an open question as to precisely why the paint affected this behavior.

C. Force and Moment Measurements Revisited: The Effect of Paint Removal and Model Polishing

The nature of the force and moment coefficient measurements mandated further study, and this was completed in the form of additional force and moment data, with close attention paid to surface roughness. A series of linear surface roughness measurements were executed on the painted model using the profilometer. The average roughness Ra was measured at 0.66 μm on the body, which compares closely with the range described in 10, 12, and 13. The maximum extent of the rough surface, described as Rt, was

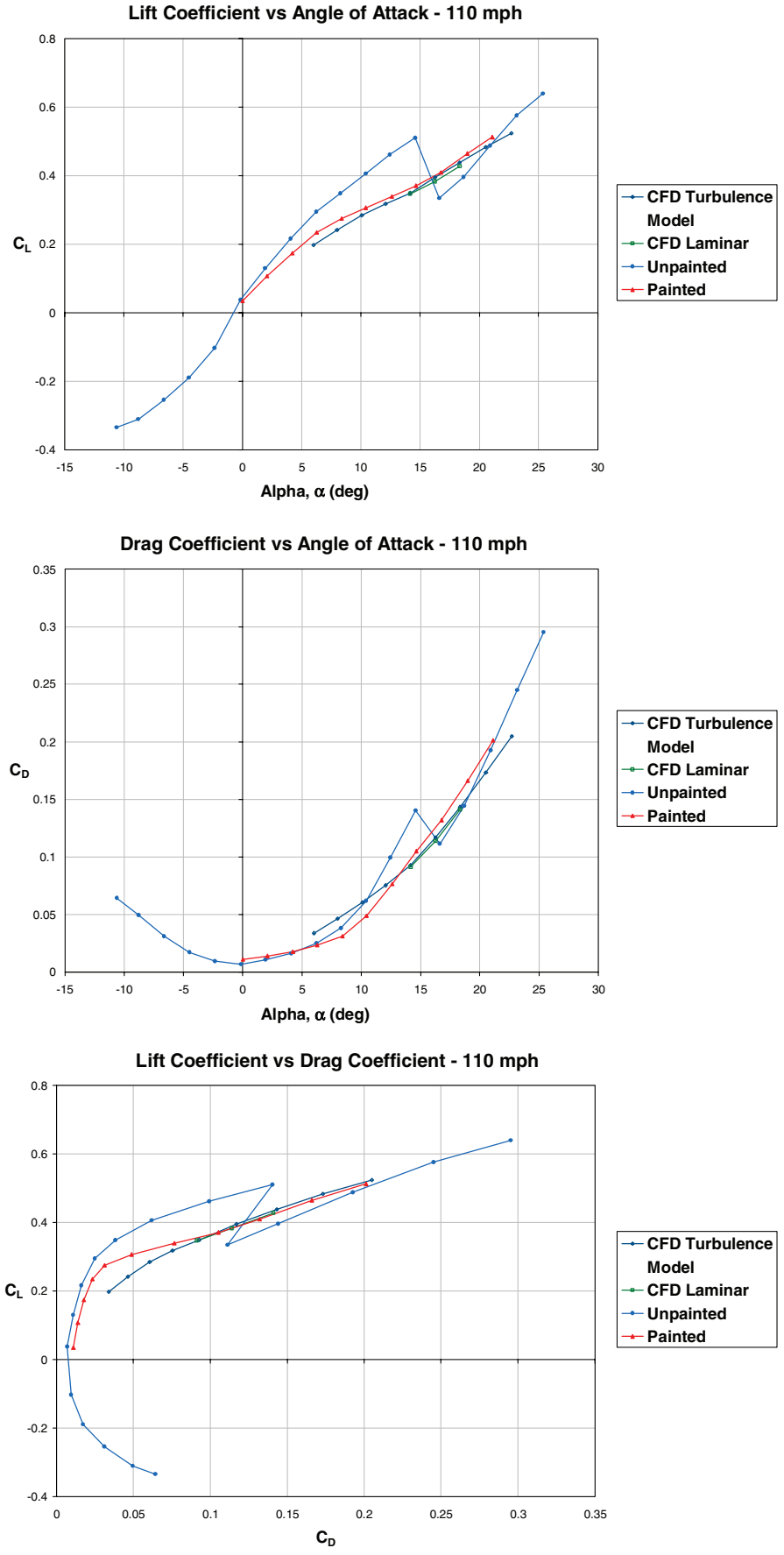

Fig. 6 Lift coefficient data as a function of angle of attack: 110 mph airspeed.

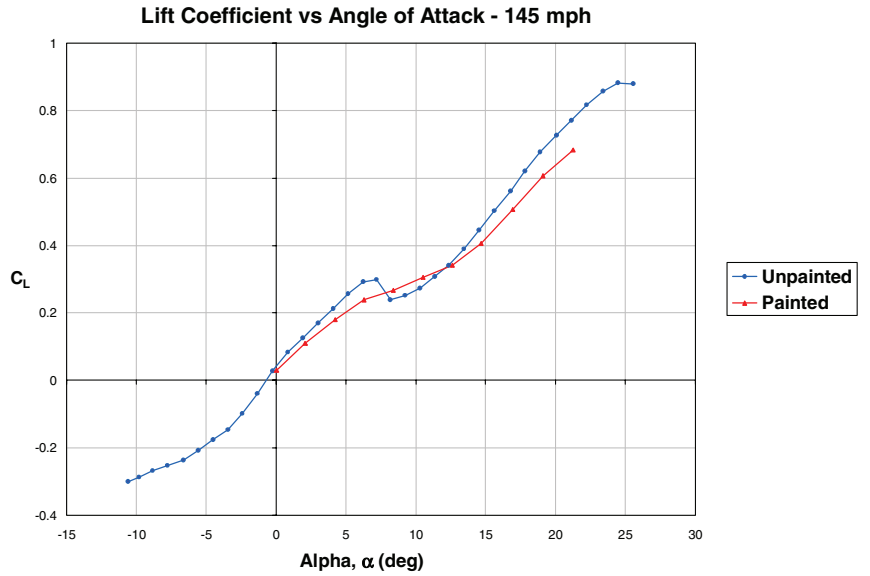

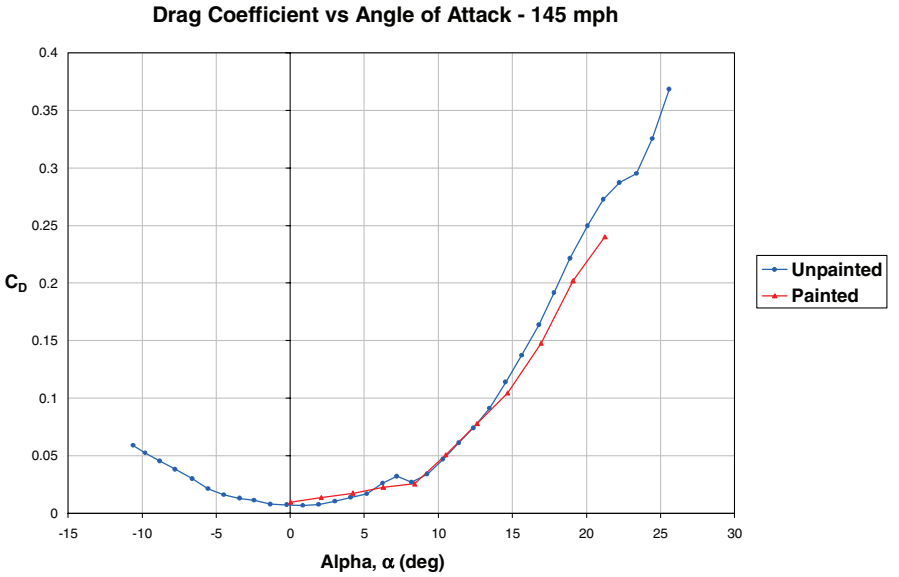

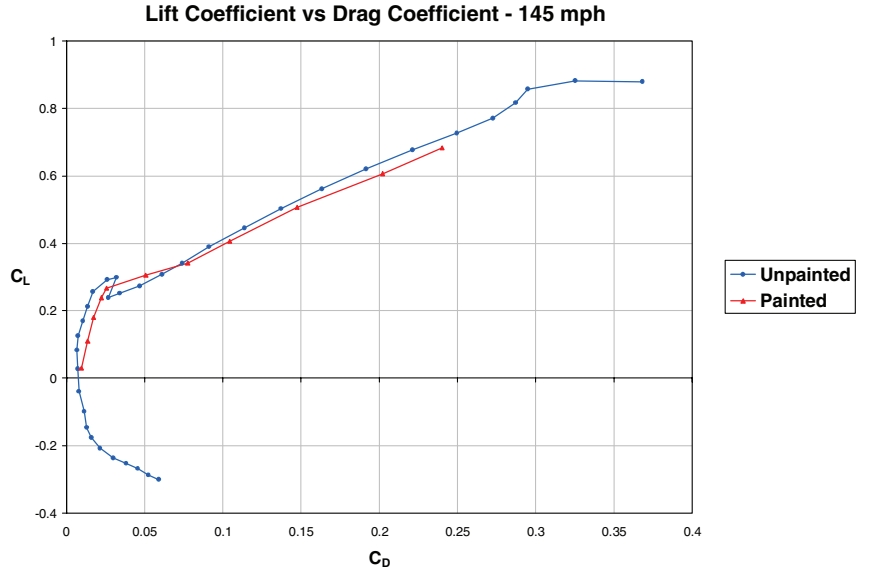

Fig. 7 Lift and drag coefficient data as a function of angle of attack: 145 mph airspeed.

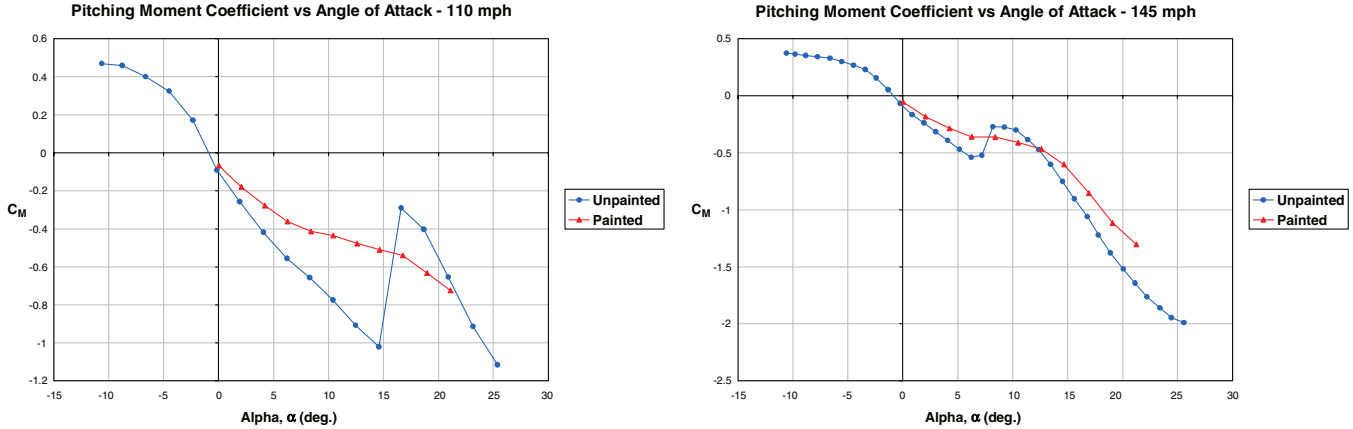

Fig. 8 Pitching moment coefficient data as a function of angle of attack for the unpainted and painted models.

6.814 μm. Similar results were seen for the roughness measured on the wing which returned a Ra of 0.62 μm and an Rt of 6.51 μm.

This level of roughness was compared to the admissible roughness for the Reynolds number of the experimental tests using the approach outlined by Schairer et al., wherein a value of 6.2 times the Ra was recommended to determine sand roughness k_s based on a literature survey. This value may then be compared to 100/(unit Re), which is described by Schlichting to be the admissible roughness criteria [11]. The value was found to yield a characteristic roughness of 4.1 μm, which was nearly an order of magnitude lower than the value of 29 μm, corresponding to a unit Re of 3.4×10^6 for the 110 mph case. This indicates that the anticipated effect of roughness would be expected to be small in this case, which is counter to the actual results.

A series of measurements were then acquired for the model under different stages of paint removal, using acetone and with the model mounted on the sting, for a single airspeed, 110 mph. The initial test of this nature was performed for the model with paint removed from the wing body junction only, including the sharp leading edge of the airfoil section in this region. Subsequently, measurements were acquired, with the model held in place on the sting, for full paint removal from the wings. Then paint was removed from the forward portion of the body. Finally, paint was removed from the tail region. The lift curves corresponding to each of these cases is shown in Fig. 12. Careful scrutiny of this plot reveals that removing the paint from only the wing body junction resulted in the reappearance of a drop in the lift coefficient, though with different characteristics from the original model. Furthermore, each time part of the paint was removed, the curve shifted to values which were slightly closer to those for the original, unpainted model. However, the lift curve did not quite return entirely to its original state, even when all the paint was removed. Removing the paint from the wing body junction region appeared to have a more pronounced effect on the $C_{L-\alpha}$ plot than did removal from other locations. Notably, by contrast to either the fully painted or original, unpainted model, stall took place gradually over an α range of 12 to 14 deg in each of these tests at 110 mph.

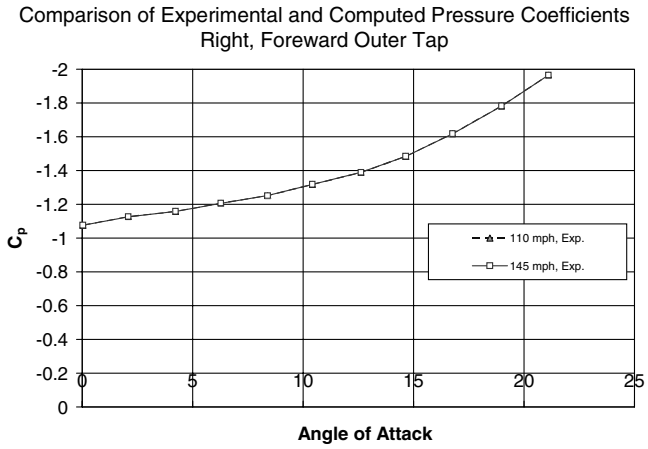

Fig. 9 Pressure coefficient data at 110 and 145 mph for the right, forward outer tap.

There is precedence in the literature for changes in model surface characteristics due to wind-tunnel testing, for example, due to sandblasting that can occur when the model is tested for prolonged periods, as was the case for the PSP runs [17]. Nevertheless, the lack of a repeatable outcome was unsatisfying. For this reason, the model was removed from the sting and polished using a commercially available stainless steel polish. Subsequently, another set of data was collected. The characteristic roughness was measured for a representative location for this polished model, and a portion of one curve is given in comparison to the painted model in Fig. 13. It is notable that the measured difference in roughness was slightly more than a factor of 2 with the polished model being smoother. The smooth models measured Ra was approximately 0.3 μm.

Force and moment data were acquired for the polished model, and the lift curve results are given in Fig. 14, in addition to several other experimental measurements for comparison. Notably, the polished model yielded a lift curve with a slope which exceeded that of the original model for the 110 mph case. Also, there was not a decrease in the lift slope corresponding to any type of clear stall event. A reasonable explanation may be that the newly polished model was smoother than the original model, but it should be noted that no roughness measurements were performed on the original, prepainted model due to the lack of anticipation of such a pronounced effect. Additional profiles were collected and are given elsewhere [19].

Summarizing this set of results, paint was removed from the model in stages. The initial removal of paint from the wing body junction region led to a reappearance of the apparent stall found for the original model. However, this apparent stall was relatively gradual in character, in contrast to that for the original, unpainted model, which exhibited sudden stall characteristics. As paint was removed from other regions of the model, the $C_{L-\alpha}$ curve shifted slightly toward values recorded for the original model. However, even when the paint for the entire model was removed, the $C_{L-\alpha}$ curve did not repeat its original data. Then the model was removed and polished, its roughness was measured, and it was then returned to its position on the sting. The lift curve acquired polished model also did not align with the original data. Rather the lift curve for the polished model increased above that of the original, unpainted data, and no stall event was witnessed. This sequence of events reinforced the conclusion that, in fact, roughness was affecting the forces acting on the model. However, a much more thorough analysis of the roughness is required to gain a full understanding of the reasons for this effect. Additional details of the paint removal process, including pictures of the partially painted model, are given in [19].

Taken as a whole, this set of results was perplexing in part because the level of roughness of even the roughest, painted model is only about 25% of the admissible roughness, based on 2-D theory. The

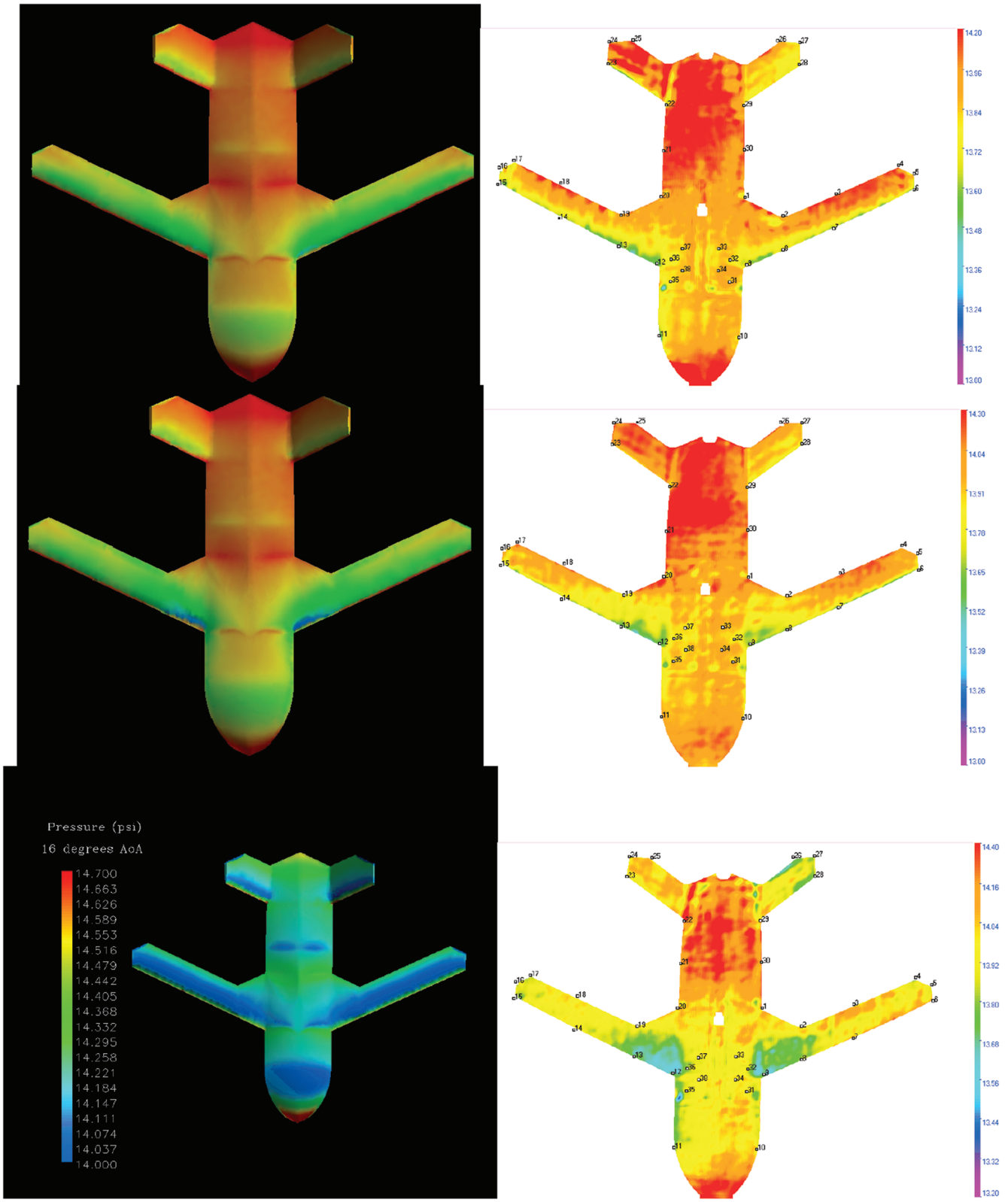

Fig. 10 Comparison of CFD (left) and PSP (right) results for $\alpha = 8$, 12, and 16 deg. The scale for CFD in the 8 and 12 case is 14.25 to 14.6 psia while the expanded scale for the 16-deg case is shown.

results appear to indicate that the general two-dimensional boundary layer theories as described by Schlichting do not necessarily apply directly without some modification due to the crossflow effects on boundary layer transition generally found in swept wing flows. Some current studies performed in this very active area of research have confirmed that the admissible roughness can be an ineffective indicator in such a circumstance. One example of this is given by the experiments of Radeztsky et al., which determined that submicron-sized roughness effects in swept wing applications had an effect on boundary layer transition. Their results showed that aerodynamic performance decreased as the surface finish of the stabilizer was improved. The research of surface roughness changes and their effects on aerodynamic performance and associated data is quite extensive, and this body of research is very active.

Alternatively, it is conceivable that the effect of the paint at the sharp leading edge of the model is affecting the development of

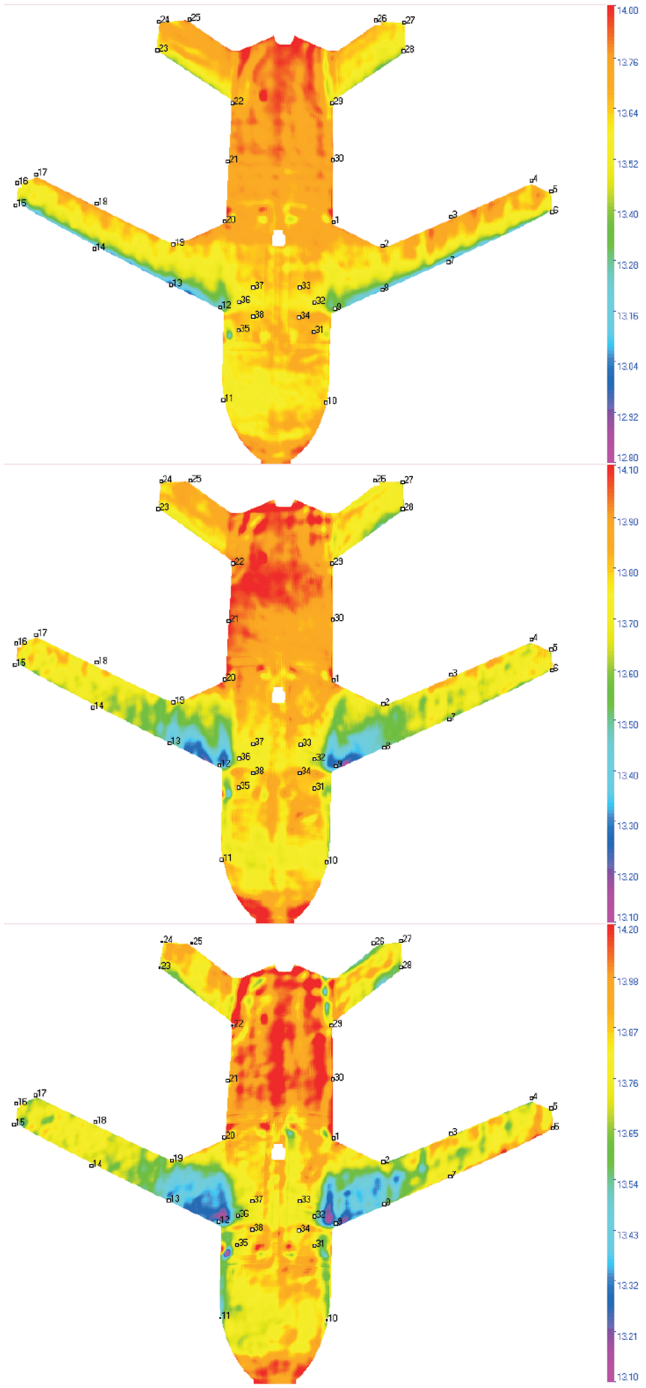

Fig. 11 PSP results for $\alpha = 8$, 12, and 16 deg for the 145 mph case. The scale on the right is given in psia.

leading edge long bubble stall. It is conceivable that the paint application in this region, though only microns thick, could have affected not only the roughness but also the effective leading edge radius of the model. If that is the primary reason for the difference in the data, the effect of surface modification via paint application, and subsequently via polishing the model, on the measured force and moment coefficients would have narrower, though still important, implications for wind-tunnel testing.

Among the studies devoted to measuring the effects of roughness caused by PSP, none to the authors' collective knowledge showed as dramatic of an effect as that reported here, which may be due in part to the fact that this study involves a relatively complex BWB model. Regardless of the effect of the paint on the leading edge, the PSP data did indicate that at sufficiently high angles of attack, there was a transition in the lift mechanism from a traditional, leading edge

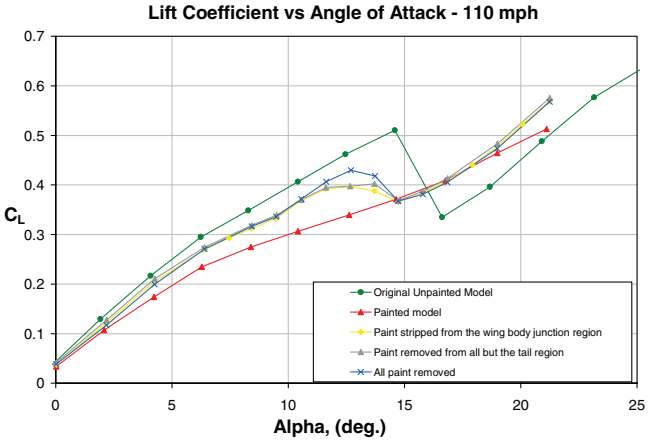

Fig. 12 Comparison of lift curves for the model with different paint coverage.

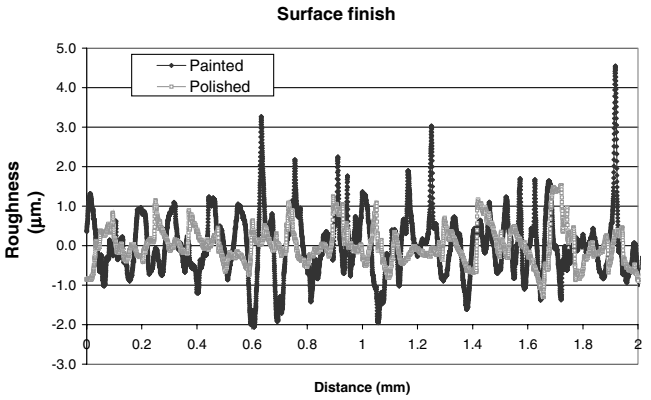

Fig. 13 Comparison of sample profilometer output for the painted model and for the polished model.

suction lift mechanism to a vortex lift mechanism near the wing body junction for the painted model. At these larger angles of attack, the force coefficient data compare rather well with that for the painted model, and it would be reasonable to assume that the same mechanism takes place for the smooth, unpainted model as well.

Interestingly, there are contrasting results for the BWB geometry in the literature, which could provide favorable comparison to the results for either the painted or unpainted model results [4,5]. In the painted model tests, the lift curve slope was shown to steadily increase through the entire angle of attack range, with a slight break in the slope seen only in the unpainted model stall region. If one takes

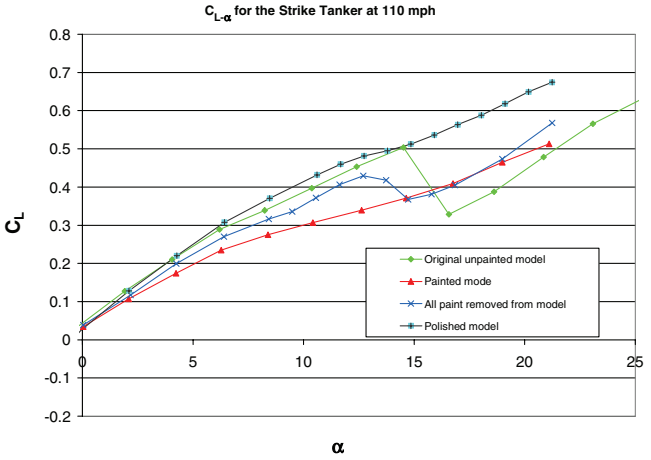

Fig. 14 Comparison of lift curves for the polished model with different paint coverage to other measured values, as indicated for 110 mph.

into account the differences in geometry, this result corresponds well to that of Katz et al., which indicates that this continuation of a positive lift curve slope is due to the lift created by the fuselage of the blended-wing body strike tanker. On the other hand the apparent stall observed for the unpainted model corresponds reasonably well to the results given by Pao et al., though there are differences, plausibly due to the different air frame geometries under consideration.

IV. Conclusions

An experimental test program was undertaken as part of a project focused on rapid design and assessment of aircraft. A 72:1 scaled-down strike tanker model was studied. Force and moment data were acquired with a six-component balance in the AFIT low-speed wind tunnel. The data were compared to CFD simulations of the model under identical conditions, and a global measurement technique (PSP) was used to more closely examine reasons for differences between forces and moments for the experiment and computation.

The testing covered airspeeds ranging from 60 to 145 mph as described in previous chapters with a focus on the 110 mph test speed, which correspond to a Mach number of 0.15 and a unit Reynolds numbers of 3.3×10^6. The initial measurements conducted for the model before the application of PSP showed substantial differences between the balance measured and CFD computed lift slopes. Moreover, a stall event was measured, the character of which the literature suggests is related to long bubble separation due to the model's sharp leading edge. This stall event revealed a strong dependence on airspeed, despite the limited range of Reynolds numbers in the test, and it is likely that the highly three-dimensional character of the model played a role in how the stall developed. Although a similar dependence on airspeed was indicated by the data given by Pao et al., the nature of this dependence in the current study appeared to be of a greater magnitude.

Subsequently, PSP was applied to the model to enable global pressure measurements with the intent that this data could be used for comparison to the CFD model. Force and moment data were taken along with the PSP, but—based on the literature survey and the expected level of admissible roughness—the effect of the paint was expected to be minimal. However, upon inspection of the results, dramatic differences were seen in the measured force and moment data before and after paint had been applied to the model. The evidence of the change in the flight characteristics is prominent in all of the lift and drag coefficient comparisons, as well as the pitching moment stability for both the 110 and 145 mph test cases. The PSP results indicated that at sufficiently large angles of attack, clearly noticeable by $\alpha = 16$ deg, a substantial low-pressure region developed on the upper surface of the model near the wing body junction, and subsequently it was deduced that this mechanism could be the generating vortex lift.

To a certain extent, the project was in part refocused toward uncovering the reason why the paint would have such a profound effect on the force and moment coefficient data. The literature suggested that surface roughness changes due to paint application could play a role. A profilometer was used to characterize the surface roughness of the model, and interestingly the roughness of the painted model was found to be below the threshhold above which one would typically expect to find an influence due to roughness, according to 2-D theory [10,11]. To quantify the effect of the surface roughness on the aerodynamics, additional force coefficient measurements were performed for the model in the wind tunnel as the paint was stripped off of sections of the model, and the effect was confirmed. Profilometer measurements indicated that the paint increased the surface roughness from Ra increased from 0.32 to 0.66 μm.

The outcome does have positive implications on the integration of rapid technology approaches related to experimental and computational fluid dynamics. Specific lessons here include the importance of using a model not only with the appropriate geometry but also with the appropriate surface conditions for testing. One important point which should be emphasized is that at an early point in the study, it appeared that the CFD model yielded a poor comparison to experimental data. In many circumstances, the computational approach would have been ruled fallible and considerable effort may have been invested into improving the CFD model. By happenstance, an experiment was performed with a slightly modified (painted) model, and the results aligned more closely with the CFD results. In this case involving a complex model, the surface condition was much more significant than one would have expected, based on the literature. A corollary to this is that a fully accurate CFD model would need to mesh volumes extremely close to the model surface to accurately account for a very smooth model. It should be emphasized that for this particular model such a condition is highly desirably for practical reasons, as the data indicate a significant improvement in the lift to drag ratio for a sufficiently smooth model.

Acknowledgments

D. A. Gebbie and M. F. Reeder would like to acknowledge the support of the U.S. Air Force Research Laboratory Air Vehicle Directorate (AFRL/VA) via a grant designated ENY 04-119. The authors would like to acknowledge the support of Bill Braisted and James Higgins of the University of Dayton Research Institute (UDRI) in their extremely helpful work supporting the model construction. The authors would like to acknowledge the assistance and diligence of Dwight Gehring of the Air Force Institute of Technology (AFIT) in coordinating and assisting with the wind-tunnel measurements. The views expressed in this article are those of the authors and do not reflect the official policy or position of the U.S. Air Force, Department of Defense, or the U.S. Government.

References

[1] Tyler, C., Braisted, W., and Higgins, J., "Evaluation of Rapid Prototyping Technologies for Use in Wind Tunnel Model Fabrication," AIAA Paper 2005-1301, Jan. 2005.

[2] Tyler, C., Reeder, M. F., Braisted, W., and Higgins, J., "Rapid Technology Focused Experimental and Computational Aerodynamic Investigation of a Strike Tanker," AIAA Paper 2004-6870.

[3] Liebeck, "Design of the Blended Wing Body Subsonic Transport," *Journal of Aircraft*, Vol. 41, No. 1, Jan. 2004, pp. 10–25.

[4] Katz, J., Byrne, S., and Hahl, R., "Stall Resistance Features of Lifting-Body Airplane Configurations," *Journal of Aircraft*, Vol. 26, No. 2, 1999, pp. 471–474.

[5] Pao, S. P., Bierdon, R. T., Park, M. A., Fremaux, C. M., and Vicroy, D. D., "Navier-Stokes Computations of Longitudinal Forces and Moments for a Blended Wing Body," AIAA Paper 2005-0045, Jan. 2005.

[6] Barlow, J., Rae, W., and Pope, A., *Low Speed Wind Tunnel Testing*, 3rd ed., Wiley, New York, 1999.

[7] Bell, J. H., Schairer, E. T., Hand, L. A., and Mehta, R., "Surface Pressure Measurements Using Luminescent Coatings," *Annual Review of Fluid Mechanics*, Vol. 33, 2001, pp. 155–206.

[8] Liu, T., Campbell, B. T., Burns, S. P., and Sullivan, J. P., "Temperature- and Pressure-Sensitive Luminescent Paints in Aerodynamics," *Applied Mechanics Reviews*, Vol. 50, No. 4, April 1997, pp. 227–246.

[9] Bell, J. H., "Applications of Pressure-Sensitive Paint to Testing at Very Low Flow Speeds," AIAA Paper 2004-0878, Jan. 2004.

[10] Schairer, E. T., Mehta, R. D., and Olsen, M. E., "Effects of Pressure-Sensitive Paint on Experimentally Measured Wing Forces and Pressures," *AIAA Journal*, Vol. 40, No. 9, 2002, pp. 1830–1838.

[11] Schlichting, H., *Boundary Layer Theory*, 7th ed., McGraw–Hill, New York, 1979.

[12] Vanhoutte, F. G., Ashill, P. R., and Gary, K. P., "Intrusion Effects of Pressure Sensitive Paint in Wind-Tunnel Tests on Wings," AIAA Paper 2000-2525, June 2000.

[13] Amer, T. R., Obara, C. J., and Liu, T., "Quantifying the Effect of Pressure Sensitive Paint on Aerodynamic Data," AIAA Paper 2003-3951, June 2003.

[14] Reed, H. L., Saric, W. S., and Arnal, D., "Linear Stability Theory Applied to Boundary Layers," *Annual Review of Fluid Mechanics*, Vol. 28, 1996, pp. 389–428.

[15] Radeztsky, R. H., Reibert, M. S., and Saric, W. S., "Effect of Isolated Micron-Sized Roughness on Transition in Swept Wing Flows," *AIAA Journal*, Vol. 37, No. 11, Nov. 1999, pp. 1370–1377.

[16] Cahill, J. F., Underwood, W. J., Nuber, R. J., and Cheesman, G. A., "Aerodynamic Forces and Loadings on Symmetrical Circular-Arc Airfoils with Plain Leading-Edge And Plain Trailing-Edge Flaps,"

NACA Rept. 1146, 1953.
[17] Hoerner, S. F., and Borst, H. V., *Fluid-Dynamic Lift*, 2nd ed., Library of Congress catalog no. 75-17441, Hoerner Fluid Dynamics, Bricktown, N.J., 1985.
[18] DeLuca, A. M., "Experimental Investigation into the Aerodynamic Performance of Both Rigid and Flexible Wing Structured Micro-Air-Vehicles," M.S. Thesis, AFIT/GAE/ENY/04-M06, Department of Aeronautics and Astronautics, Air Force Institute of Technology (AU), Wright–Patterson AFB, OH, March 2004.
[19] Gebbie, D. A., "Experimental Study Of The Subsonic Aerodynamics Of A Blended Wing Body Air Vehicle With A Focus On Rapid Technology Assessment," M.S. Thesis, AFIT/GAE/ENY/04-M06, Department of Aeronautics and Astronautics, Air Force Institute of Technology (AU), Wright–Patterson AFB, OH, March 2004.